

Variation of Nominal Contact Pressure with Time during Sliding Wear^{*}

O. O. Ajayi and R. A. Erck

Energy Technology Division
Argonne National Laboratory
Argonne, IL 60439

Phone (630) 252-9021
Fax (630) 252-4798
e-mail: ajayi@anl.gov

The submitted manuscript has been created by the University of Chicago as Operator of Argonne National Laboratory under Contract No. W-31-109-ENG-38 with the U.S. Department of Energy. The U.S. Government retains for itself, and others acting on its behalf, a paid-up, nonexclusive, irrevocable worldwide license in said article to reproduce, prepare derivative works, distribute copies to the public, and perform publicly and display publicly, by or on behalf of the Government.

January 2001

Manuscript of paper to be presented at 2001 International Joint Tribology Conference
October 22-24, 2001, San Francisco.

^{*} Work supported by the U.S. Department of Energy, Office of Transportation Technology, under Contract W-31-109-Eng-38.

Variation of Nominal Contact Pressure with Time during Sliding Wear*

O. O. Ajayi and R. A. Erck

Energy Technology Division
Argonne National Laboratory
Argonne, IL 60439

ABSTRACT

The variation of nominal contact pressure with sliding distance/time during sliding wear of a nonconformal contact was analyzed from experimental data available in the open literature and data from tests we conducted with five materials under unlubricated, solid-lubricated, and oil-lubricated conditions. All of the data are from specimens that were in ball-on-flat test configuration in reciprocating and unidirectional sliding. In all cases, the "instantaneous" nominal contact pressure decreased very rapidly during the first few meters of sliding as wear occurred. For all of the examined cases, the nominal contact pressure can be empirically related to the sliding distance/time by an inverse power function. The relationship between the pressure and the sliding distance involves two constants. One is determined by the total amount of wear on the ball, whereas the other is dependent on the ball wear rate. An attempt was made to extend the analysis to asperity-level contacts. The established relationship between the nominal contact pressure and distance/time, even though empirical, will facilitate better understanding, interpretation, and prediction of wear and other changes that occur at a sliding contact interface.

*Work supported by the U.S. Department of Energy, Office of Transportation Technology, under Contract W-31-109-Eng-38.

INTRODUCTION

The vast majority of laboratory bench top friction and wear tests are conducted with nonconformal contact geometries. These geometries are often in the form of “point” contacts, wherein a ball or hemispherical tip pin is loaded against a flat surface – usually called pin-on-disc, ball-on-flat, or other similar names. Point contacts are also created in cylinder-on-cylinder contacts. In the “line” contact, a cylinder is loaded against a flat surface with its axis parallel to the flat surface or two cylinders with their axes parallel to each other. Although these are classified as point and line contacts, there are finite circular and rectangular areas of contact, respectively. These areas can be calculated by using Hertzian theory.

Nonconformal contact configurations are attractive for testing for two main reasons, namely ease of alignment and absence of edge loading. Investigators conducting wear tests can readily understand the enormous difficulty of aligning a flat-ended pin on a flat disc. Even a slight misalignment will produce a nonuniform rate of wear across the pin contact area.

In wear tests that use nonconformal contact configuration, the nominal contact area increases as wear occurs over time. The result is a decrease in nominal contact pressure, by as much as orders of magnitude, as the test progresses. Although this is well recognized, most authors will often provide only the initial Hertzian contact pressure for their test conditions. In many cases, the authors will proceed to base their subsequent analysis and explanations of their experimental results and observations on the initial contact stress. Such an approach could be very misleading, because the amount of time

the contact spends under Hertzian conditions is very short when compared with the total test time.

The nature and extent of damage and wear that occurs at the sliding contact interface are determined by the imposed contact stresses and the concomitant frictional heating. The magnitudes of both contact stresses and frictional heating are proportional to the nominal contact pressure. For instance, in a sliding elastic contact of smooth surfaces of a ball-on-flat solids, the maximum tensile stress (σ_{\max}) at the trailing edge of the contact is given by $\left(\frac{1-2\nu}{3} + \frac{4+\nu}{8}\pi\mu\right)P_o$ where ν is the Poisson ratio, μ is the friction coefficient, and P_o is the maximum contact pressure [1].

Also a shear stress is imposed at the interface; its value is dependent on maximum contact pressure. Similarly, the rate of frictional heat generation per unit contact area (q) is given as $q = \mu P_{av} S$, where P_{av} is the average contact pressure and S is the sliding speed. The analysis and equations for stresses and heating are also valid for rough surfaces if one assumes a model of spherical shaped asperities. Then, the damage and wear will begin at the asperity level, and stresses and temperature distribution can be superposed on the macrocontact geometry values. At both micro- and macro-levels, the contact pressure will decrease as wear occurs because of increase in contact area.

To develop a better understanding of the damage and wear mechanisms that occur at the sliding-contact interface, it is essential that we know the variation of contact pressure with time (sliding distance). This is particularly more so, for the quantification and prediction of wear amount or extent of surface damage. The goal of this paper is to experimentally establish a time variation of nominal contact pressure during sliding

contact of a nonconformal contact. Initial analysis conducted on the data of Mecklenburg [2] was augmented with wear tests we conducted with various materials under different sliding contact conditions.

EXPERIMENTAL DETAILS

Sliding wear tests were conducted with a pin-on-flat contact geometry in reciprocating sliding motion. A detailed description of the testing device has been previously given [3,4]. The pins were made from a cylindrical rod of 15 mm length and 8 mm diameter. One end of the pin was rounded to form a hemispherical cap with radius of curvature of 127 mm. The flat specimens are made of rectangular blocks of nominal dimension of 50 x 20 x 6.5 mm. The pin, firmly attached to the loading arm, is moved in reciprocating motion across the stationary flats.

Five materials were tested in self-mating contact combinations. Table 1 shows these materials and their relevant elastic properties. For all the tests, both the pin and the flat specimen surfaces were polished to a final finish of about $0.08 \mu\text{m } R_a$. Unlubricated sliding wear tests were conducted with a normal load of 10 N, reciprocating frequency of 1 Hz, and a stroke length of 25 mm, giving an average sliding speed of 0.05 m/s. Solid-lubricated tests were conducted with Si_3N_4 at loads of 10 and 50 N. This was accomplished by coating the Si_3N_4 disc with an $\approx 1.5 \mu\text{m}$ thick layer of Ag (solid lubricant) by the ion-beam-assisted deposition (IBAD) technique. Oil-lubricated tests were also conducted for four of the materials at a normal load of 50 N. Fully flooded lubricated contact was created by submerging the flat specimen in oil during the test. A fully formulated polyolester based synthetic oil was used as the lubricant. All of the tests were performed under ambient room conditions of $\approx 23^\circ\text{C}$ temperature and 30-50% relative humidity

The tests were interrupted after 100, 250, 500, 1000, 2000, 3000, 4000, and 5000 cycles and the dimension of the pin wear scar was measured with an optical microscope. Nominal contact pressure was then calculated from the pin scar dimension. It was observed that in general, the shape of the wear scar was circular or elliptical. For circular scars, the nominal contact pressure (P_n) is given as $P_n = W/\pi r^2$, where W is the normal force and r is the wear scar radius. For elliptically shaped scars, $P_n = W/\pi ab$, where a and b are the half-lengths of the major and minor axes respectively.

RESULTS AND DISCUSSION

The calculated initial mean Hertzian contact pressures for the materials we tested are shown in Table 2. Equations for the calculation can be found in most mechanics books [e.g. Ref. 5]. For the contact configuration of a ball or hemispherical pin statically loaded onto a flat surface, the radius of point contact circle a is given as

$$a = \left(\frac{3WR}{4E^*} \right)^{\frac{1}{3}} \quad (1)$$

where W is the normal load, R is the relative curvature defined as $1/R = 1/R_1 + 1/R_2$; R_1 and R_2 are the radius of curvature of bodies 1 and 2 respectively. (For the ball-on-flat contact, $R_2 = \infty$, thus R is the ball radius.)

E^* is the reduced modulus, defined by the equation

$$\frac{1}{E^*} = \left(\frac{1 - \nu_1^2}{E_1} + \frac{1 - \nu_2^2}{E_2} \right) \quad (2)$$

where ν_1 and ν_2 are Poisson ratios for bodies 1 and 2 respectively, and E_1 and E_2 are their Young's moduli.

The maximum contact pressure P_0 at the axis of contact is given as

$$P_o = \frac{3W}{2\pi a^2} = \left(\frac{6WE'^2}{\pi^3 R^2} \right)^{\frac{1}{3}} \quad (3)$$

The mean pressure over the contact area P_m is given by

$$P_m = \frac{2}{3} P_o = \frac{W}{\pi a^2} \quad (4)$$

The pressure distribution over the contact area is given as

$$P = P_o \left(1 - \left(\frac{r}{a} \right)^2 \right)^{\frac{1}{2}} \quad (5)$$

During sliding, wear occurs and the contact area increases resulting in reduction of the nominal contact pressure. A plot of the variation of the measured nominal contact pressure with sliding distance/time during the unlubricated sliding tests with five different material pairs is shown in Figure 1. The figure shows a rapid decrease in contact pressure, by about two orders of magnitude, over the first 25 m of sliding. Beyond the initial drop, there was only a modest decrease for the remaining duration of the test. The only exception to this rapid drop was the TZP-ZrO₂, where the decrease was more gradual throughout the duration of the test. This behavior of ZrO₂ could be due to the impact of transformation-induced plasticity on the wear mechanism at the contact interface.

The tetragonal phase of ZrO₂ can undergo a stress-induced martensitic transformation to monoclinic phase. This phase transformation is accompanied by about 5% volume increase, producing a compressive residual stress. The phase transformations have been observed during wear of tetragonal-phase-containing ZrO₂ material, and

associated with the high wear resistance in such materials [6]. The phase transformation is expected to be more pronounced under higher contact pressure at the initial stage of the test. The resultant improvement in wear resistance produced the observed lower rates of wear and decrease in the nominal contact pressure.

The plot in Figure 2a is the data of Mecklenburg [2] for sliding wear tests of M10 steel contact pairs in a ball-on-disc contact configuration with a solid CF_x coating on the disc. In essence, the test materials were lubricated with a solid-lubricant coating. Figure 2b shows the contact pressure variation for the solid-lubricated (Ag-coated) Si_3N_4 in sliding contact. By inspection, it is clear that the variation of nominal contact pressure with sliding distance in these solid-lubricated tests follows the same trend as dry unlubricated tests.

Figure 3 shows the variation of nominal contact pressure with sliding distance in oil-lubricated tests. The contact pressure followed the same trend as the dry test, but the extent of decrease is less than that in dry tests by one order of magnitude. This definitely reflects the fact that the amount of wear in lubricated contacts is less than the amount of wear in unlubricated ones. Furthermore, the fully formulated oil used as lubricant probably contains some chemical antiwear additives and thus will reduce the amount of wear even more. In oil-lubricated Si_3N_4 and ZrO_2 ceramics, the contact pressure drop was more gradual than in steel, but continued throughout the test such that by the end of test, there was a larger total decrease than in the steel tests. This may be due to the fact that the additives package in the oil that works in reducing wear in steel is not having the same effect in ceramics.

In all of the examined cases, the variation of nominal contact pressure with sliding distance or time can be expressed in the empirical relationship of an inverse power law form:

$$P_n = \beta P_m d^{-k} \quad (6)$$

Where P_n is the "instantaneous" nominal contact pressure (Pa), β and k are constants, P_m is the initial mean Hertzian contact pressure, and d is the sliding distance (m). The values of constants β and k for various materials tested under different test conditions are shown in Table 3.

The fact that all of the analyzed data showed an inverse power function relationship between the “instantaneous” contact pressure and sliding distance/time may suggest a general applicability of the relationship. All of the physical significance of the correlating constants β and k cannot be fully ascertained at this time. For an empirical analysis, as in this case, the larger the body of analyzed data, the higher the level of confidence in inferences derived from such an analysis. Nevertheless, the parameter β appears to be a measure of the nearly steady value of the nominal contact pressure after the initial rapid decrease in the early stages of wear. Its value is dependent on the total amount of wear during the test. One would then expect all of the factors and material properties that influence the amount of wear to determine the value of β . Similarly, the other parameter, k , appears to be connected with the rate of decrease of the nominal contact pressure in the early stages of the test. Thus, the value of k is dependent on the wear rate during the early stages (run-in) of the test. It is noted that when $k = 0.5$, the wear rate is steady, when $k < 0.5$, wear rate decreases with time, and when $k > 0.5$, wear rate increases with time. Again, factors that influence the wear rate (including the wear mechanism) during run-in at the early stages of testing will affect the value of k .

Further data analysis is required to determine the range of values of β and k and their physical significance.

The analysis can be extended to the micro level of asperity contact. If we assume uniformly sized and spherically shaped asperities, the initial contact area between a pair of asperities will occur over a circular area. Average asperity contact pressure can be calculated by dividing the applied load by the total area of all the contacting asperity pairs. This real area of contact of the asperities is much smaller than the nominal area of contact, and for most materials, the asperity contact pressure will exceed the yield pressure of the material. For brittle materials with limited plasticity, fracture may occur at the asperities instead of plastic deformation. These processes can be incorporated into the asperity contact pressure analysis by setting a work-hardened corrected yield pressure or the asperity fracture pressure as the upper limit for contact pressure. For a constant load contact, and with an upper limit of the contact pressure set, the initial area of contact of asperities can be estimated.

When sliding is imposed on a constant load contact, wear will occur at the tips of contacting asperities, thereby increasing their contact area. The result will be a rapid drop in the contact pressure as in the case of nominal contact pressure. Focusing on a single asperity on which wear is occurring, we can assume that the asperity contact pressure (P_{ai}) during sliding wear follows the same behavior as the nominal contact pressure (with the initial yield pressure set to the work-hardened yield pressure), and can be expressed as

$$P_{ai} = \beta_a P_y d^{-k_a} \quad (7)$$

Where P_y is the yield pressure, and β_a and k_a are fitting parameters for asperity contacts. This assumes that the real (asperities) area of contact increases as wear occurs during

sliding contact. Of course, in real surfaces, asperities vary in size and shape distribution, thereby making the calculation of asperity contact pressure mathematically involved.

An alternate approach to estimating asperity contact pressure is to assume a continuously random contact and collisions between asperities of various sizes and shapes. It is further assumed that contact occurs in such a way that the ratio of real area of contact (A_r) to the nominal area of contact (A_n) is always constant for a given load. The average “instantaneous” asperity pressure as a function of time can then be estimated by simply multiplying Eq. 6 by the ratio of nominal to real areas of contact. The expression could be written as

$$P_{ai} = (A_n/A_r) \beta P_m d^{-k} \quad (8)$$

The establishment of an empirical relationship between the nominal contact pressure and sliding distance/time, as done in this paper will certainly enhance better understanding and interpretation of wear test data. It will facilitate more accurate computation and a more realistic assessment of dynamic changes that occur during a sliding wear test. The magnitude of various stress components and the rate of frictional heat input into the contact area can now be estimated as a function of test time. Currently, computer codes and simple expressions are available to calculate contact stresses and temperatures during sliding contact [e.g Ref. 7]. These analyses are often based on the initial Hertzian contact pressure. By incorporating into the analyses the variation of nominal pressure with time, as set forth in this paper, more realistic stress state and temperature distributions can be calculated. Changes in wear mechanisms and

wear rates can then be more accurately connected with changes in the driving forces for the changes.

Perhaps the most significant result of the establishment of this pressure-time variation during sliding wear tests, is the possibility of more accurately predicting and modeling wear rates. Predictive insight into wear mechanism changes could also be gained. The usual current practice in wear testing is to provide the normal contact load and perhaps initial contact pressure. Investigators will often base their subsequent analysis and quantification on these initial parameters. With a more accurate calculation/estimation of the contact stresses and temperature at the sliding contact interface as a function of time, a more accurate calculation of wear rates as a function of time is possible. This will facilitate a better correlation of sliding-wear data with component performance.

CONCLUSIONS

The variation of nominal contact pressure with sliding distance/time was determined during sliding wear tests with a pin-on-flat contact configuration. Data from the literature were supplemented with tests of five materials (three ceramic and two metallic) under unlubricated, solid-lubricated, and oil-lubricated conditions. In all cases, a rapid decrease in the nominal contact pressure occurred during the first 5-10 m of sliding. The initial drop was followed by a more gradual decrease, eventually reaching a nearly steady value. In all cases, the nominal contact pressure varies with the sliding distance according to an inverse power relationship. The establishment of this relationship between the contact pressure and sliding distance/time will facilitate a better

estimation of the components of contact stresses and surface temperature rise due to frictional heating. This will lead to better understanding and prediction of wear and other tribological phenomena that may occur during wear tests. A better connection between laboratory bench test results from, for example, the common pin-on-disc machine and tribological hardware field performance could be enhanced by this knowledge about contact pressure variation during testing. Because the present analysis is primarily empirical, more data analysis is required to increase the confidence level in the general applicability of the relationship – a challenge for the entire tribological community.

REFERENCES

1. M. T. Langier, *J. Mater. Sci. Lett.*, **5** (1986), 253-254.
2. K. R. Mecklenburg, *ASLE Trans.*, **17** (1974), 149-157.
3. A. Erdemir, G. R. Fenske, F. A. Nichols and R. A. Erck, *STLE Trib. Trans.*, **33** (1990), 511-518.
4. O. O. Ajayi, A. Erdemir, R. H. Lee and F. A. Nichols, *J. Am. Ceram. Soc.*, **76** (1993), 511-517.
5. K. L. Johnson, "Contact Mechanics", Cambridge University Press, Cambridge, UK (1985).
6. V. Aronov, *ASLE Trans.*, **30** (1987), 100-104.
7. S. C. Lim and M. F. Ashby, *Acta Metall.*, **35** (1987), 1-24.

Table 1: Elastic properties of tested materials.

Material	Hardness (GPa)	Young's Modulus (GPa)	Poisson Ratio
SiC	28.0	410	0.14
Si ₃ N ₄	17.4	294	0.28
ZrO ₂	13.2	206	0.31
52100 Steel	8.4	200	0.30
M50 Steel	8.0	200	0.30

Table 2: Initial mean Hertzian contact pressure for various material Pairs at 10- and 50- N normal force

Material Pair	Contact Pressure (MPa)	
	10 N	50N
SiC	118	198
Si ₃ N ₄	96.7	165
ZrO ₂	77.3	132
52100 Steel	75.4	129
M50 Steel	75.4	129

Table 3: Values of curve fitting constants β and k for various material pairs.

Material Pair	Dry		Solid-lubricated		Oil-Lubricated	
	β	k	β	k	β	k
SiC	0.025	0.323	-	-	-	-
Si ₃ N ₄	0.066	0.429	0.08	0.446	0.288	0.346
ZrO ₂	0.171	1.466	-	-	0.161	1.207
52100 Steel	0.099	0.568	-	-	0.331	0.221
M50 Steel	0.0386	0.331	-	-	0.294	0.236

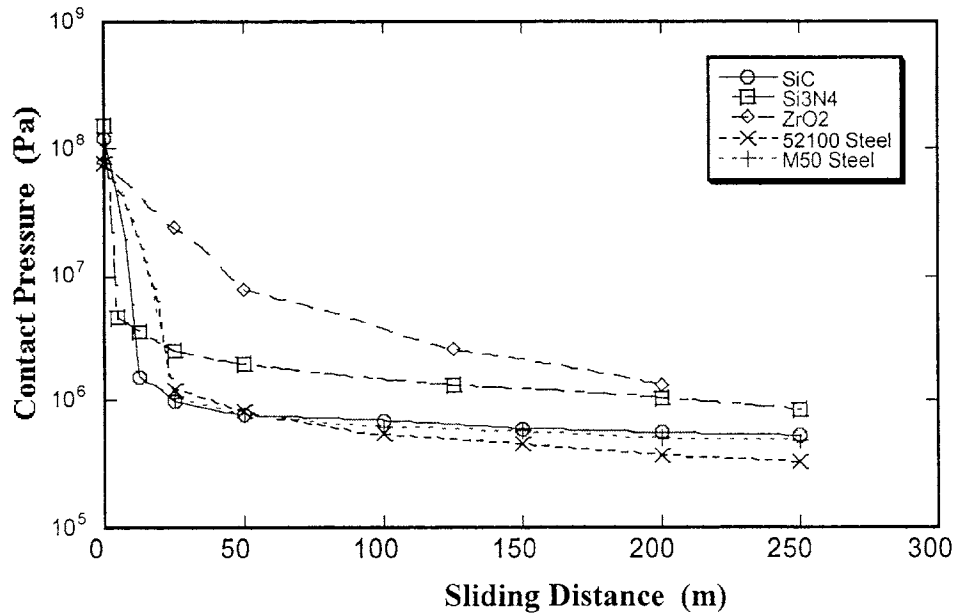
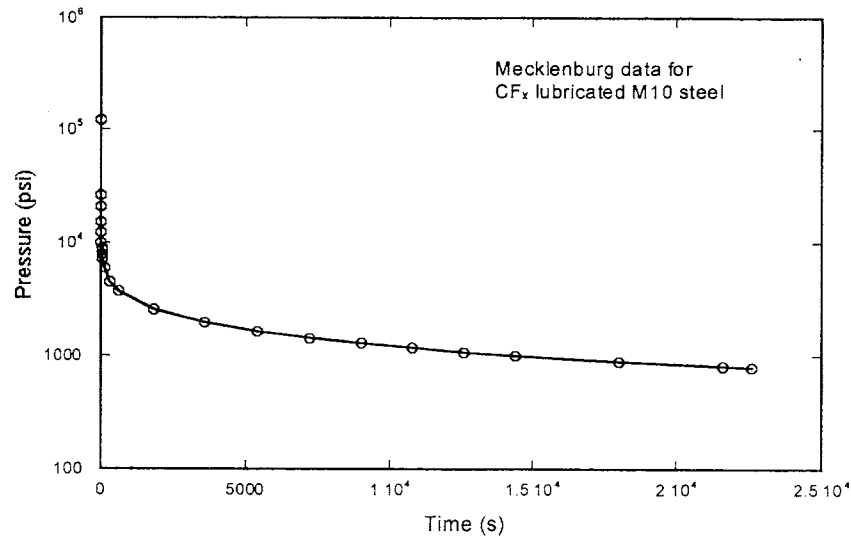
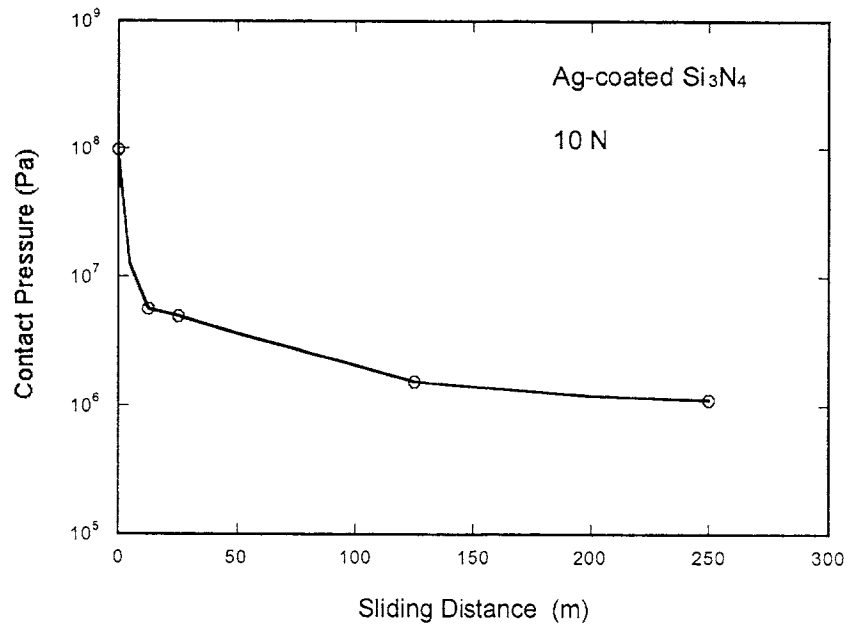


Figure 1: Variation of nominal contact pressure with sliding distance during dry wear tests of various materials



(a)



(b)

Figure 2: Nominal contact pressure variation with sliding distance in solid-lubricated tests: (a) CF(x)-lubricated M10 steel [2] (b) Ag-lubricated Si₃N₄

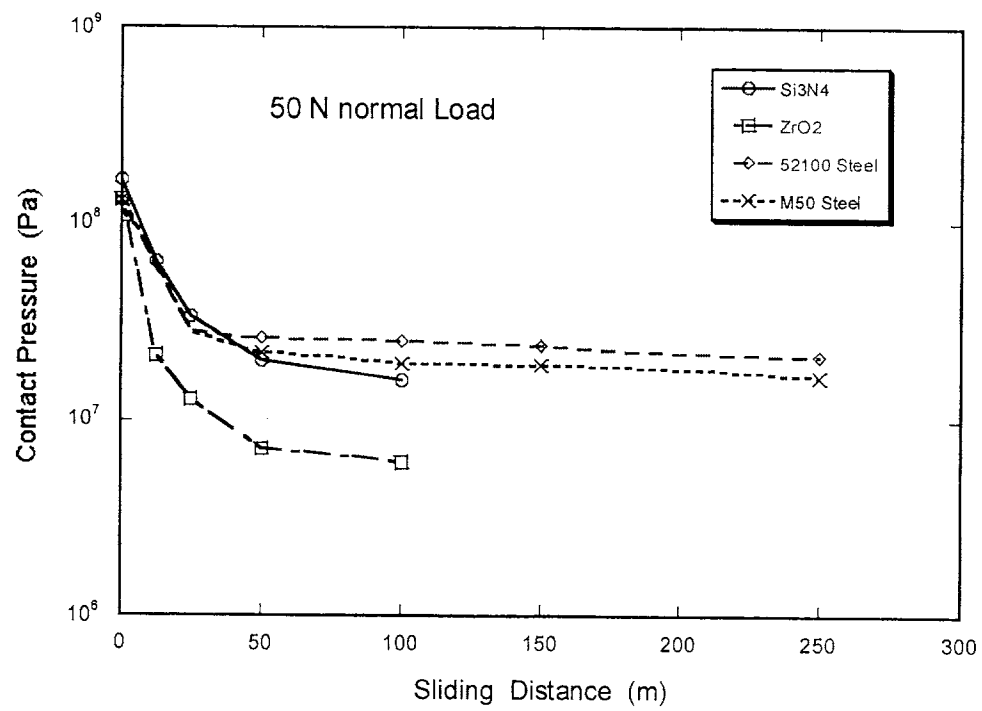


Figure 3: Nominal contact pressure variation with sliding distance in oil-lubricated tests